



Targeting copper(II)-induced oxidative stress and the acetylcholinesterase system in Alzheimer's disease using multifunctional tacrine-coumarin hybrid molecules



Slavka Hamulakova^a, Patrik Poprac^b, Klaudia Jomova^c, Vlasta Brezova^b, Peter Lauro^c, Lenka Drostinova^c, Daniel Jun^d, Vendula Sepsova^d, Martina Hrabínova^d, Ondrej Soukup^e, Pavol Kristian^a, Zuzana Gazova^{f,g}, Zuzana Bednarikova^{a,f}, Kamil Kuca^{e,h}, Marian Valko^{b,h,*}

^a Institute of Chemistry, Faculty of Science, P. J. Safarik University, SK-041 67 Kosice, Slovakia

^b Department of Physical Chemistry, Faculty of Chemical and Food Technology, Slovak University of Technology in Bratislava, SK-812 37 Bratislava, Slovakia

^c Department of Chemistry, Faculty of Natural Sciences, Constantine the Philosopher University, SK-949 74 Nitra, Slovakia

^d Department of Toxicology and Military Pharmacy, Faculty of Military Health Sciences, University of Defence, CZ-500 01 Hradec Kralove, Czech Republic

^e Biomedical Research Centre, University Hospital Hradec Kralove, CZ-500 05 Hradec Kralove, Czech Republic

^f Department of Biophysics, Institute of Experimental Physics, Slovak Academy of Sciences, SK-041 67 Kosice, Slovakia

^g Department of Medical and Clinical Biochemistry, Faculty of Medicine, P. J. Safarik University, SK-040 11 Kosice, Slovakia

^h The Center for Basic and Applied Research, University Hradec Kralove, Hradec Kralove, CZ-500 01, Czech Republic

ARTICLE INFO

Article history:

Received 24 February 2016

Received in revised form 17 April 2016

Accepted 4 May 2016

Available online 5 May 2016

Keywords:

Free copper

Tacrine-coumarin hybrids

Alzheimer's disease

Oxidative stress

DNA damage

ABSTRACT

Alzheimer's disease is a multifactorial disease that is characterized mainly by Amyloid- β (A- β) deposits, cholinergic deficit and extensive metal (copper, iron)-induced oxidative stress. In this work we present details of the synthesis, antioxidant and copper-chelating properties, DNA protection study, cholinergic activity and amyloid-antiaggregation properties of new multifunctional tacrine-7-hydroxycoumarin hybrids. The mode of interaction between copper(II) and hybrids and interestingly, the reduction of Cu(II) to Cu(I) species (for complexes Cu-5e-g) were confirmed by EPR measurements. EPR spin trapping on the model Fenton reaction, using 5,5-dimethyl-1-pyrroline *N*-oxide (DMPO) as a spin trap, demonstrated a significantly suppressed formation of hydroxyl radicals for the Cu-5e complex in comparison with free copper(II). This suggests that compound 5e upon coordination to free copper ion prevents the Cu(II)-catalyzed decomposition of hydrogen peroxide, which in turn may alleviate oxidative stress-induced damage. Protective activity of hybrids 5c and 5e against DNA damage in a Fenton system (copper catalyzed) was found to be in excellent agreement with the EPR spin trapping study. Compound 5g was the most effective in the inhibition of acetylcholinesterase (*hAChE*, $IC_{50} = 38$ nM) and compound 5b was the most potent inhibitor of butyrylcholinesterase (*hBuChE*, $IC_{50} = 63$ nM). Compound 5c was the strongest inhibitor of A- β_{1-40} aggregation, although a significant inhibition (>50%) was detected for compounds 5b, 5d, 5e and 5g. Collectively, these results suggest that the design and investigation of multifunctional agents containing along with the acetylcholinesterase inhibitory segment also an antioxidant moiety capable of alleviating metal (copper)-induced oxidative stress, may be of importance in the treatment of Alzheimer's disease.

© 2016 Elsevier Inc. All rights reserved.

1. Introduction

Alzheimer's disease (AD) is a chronic neurodegenerative disorder which is characterized by various symptoms including a loss of cognitive capacity [1]. The pathogenesis of Alzheimer's disease has been linked to a deficiency of the neurotransmitter acetylcholine in the brain, which maintains communication between neurons [2]. A

deficiency of acetylcholine is caused by the disturbed (aberrant) activity of an enzyme, acetylcholinesterase (AChE), which converts acetylcholine into the inactive metabolites, choline and acetate. The principal therapy for patients with Alzheimer's disease consists of the application of centrally acting acetylcholinesterase inhibitors to compensate for the depletion of acetylcholine in the brain, for which purpose, Tacrine and its derivatives are the most important drugs used [3–5].

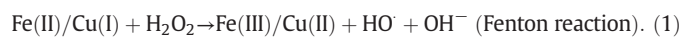
Another important biomolecule in Alzheimer's disease is Amyloid- β (A- β), a peptide containing 36–43 amino-acids, which tends to bunch up initially into small clusters that are still soluble and can move freely in the brain and finally into the amyloid plaques that are hallmarks of Alzheimer's diseases [6]. The neurotoxic effects of A- β probably stem

* Corresponding author at: Department of Physical Chemistry, Faculty of Chemical and Food Technology, Slovak University of Technology in Bratislava, SK-812 37 Bratislava, Slovakia.

E-mail address: marian.valko@stuba.sk (M. Valko).

from its ability to cause oxidative stress and its accumulation in the form of deposits in the brain. In addition, A- β possesses a high affinity for metal ions such as zinc, copper and iron, which may in turn promote its aggregation [7]. Numerous studies of Alzheimer's patients have confirmed the presence of oxidative damage to A- β which is directly linked with the presence of free (unbound) Cu and Fe, which are redox-active metals.

Significant progress in the precise quantification of redox active metals such as iron and copper, and the non-redox metal, zinc, in the brain-tissue of Alzheimer's patients, has been made by the application of three unique physical techniques, i.e. scanning transmission ion microscopy, Rutherford back scattering spectrometry and particle induced X-ray emission in conjunction with a high energy proton microprobe [8]. The results obtained have revealed an increased concentration of metals in the amyloid plaques in tissues taken from Alzheimer's patients, compared with the surrounding tissues. The level of iron in amyloid plaques was determined to be nearly double, while those of copper and zinc were found to be nearly triple those in the surrounding tissue. These data are consistent with a catalytic role for redox-active transition metal ions (Cu and Fe) in the formation of oxidizing species which in turn contribute to the occurrence of various signs of oxidative stress in brain tissues, and may be taken to support a mechanism in which the redox-metals catalyse the formation of free radicals (hydroxyl radicals, HO \cdot), mainly via decomposition of hydrogen peroxide (Fenton reaction), which is continuously produced under in vivo conditions in mitochondria (Eq. 1) [9]



Hydroxyl radicals are extremely reactive and may cause damage to all important biomolecules in the brain, including DNA [9]. The major signs of an oxidative stress component in AD brains include increased lipid peroxidation, which was substantiated by an elevated concentration of 4-hydroxynonenal [10]. In addition, increased levels of oxidized DNA and proteins, a diminished energy metabolism, an inhibited synthesis of cytochrome c oxidase, increased levels of malondialdehyde, and the observation of advanced glycation end-products (AGEs) have all been observed in AD brains [11].

Despite the fact that the oxidative stress plays an important role in the etiology of Alzheimer's disease, a previous major emphasis has been placed upon the development of compounds that function as cholinesterase inhibitors, probably the most studied of which is Tacrine. Tacrine (1,2,3,4-tetrahydroacridin-9-amine) is both a centrally acting anticholinesterase and an indirect cholinergic agonist and was the first centrally acting cholinesterase inhibitor that was approved for the treatment of Alzheimer's disease.

In view of the importance of targeting the oxidative stress component in AD, the design of multifunctional agents containing an antioxidant functionality is of great importance. Indeed, there has been a more recent gradual direction taken toward the development and testing of dual functioning drugs (hybrids), which contain both an "acetylcholinesterase inhibitory" moiety and an "oxidative stress suppressing" moiety [12–14].

Coumarins are a widespread class of natural phenolic compounds, which contain a benzene ring fused with an α -pyrone ring, and exhibit a wide range of biological activities, including free radical scavenging [15–17]. We propose to employ the coumarin structure as an oxidative stress suppressing moiety in dual functioning drugs to be used against AD. Recent studies have demonstrated the enzyme-inhibiting [18,19] and antioxidant activities of coumarins [20,21], while a large number of coumarin derivatives have been found to possess tissue-protective antioxidant properties which not only are a result of scavenging reactive nitrogen species (RNS) and reactive oxygen species (ROS) per se, but of suppressing their formation, a priori [22]. In particular, hydroxyl-substituted coumarins act as effective redox-active metal chelators, free radical scavengers and powerful chain-breaking antioxidants,

while other coumarins have been demonstrated to be potent monoamine oxidase (MAO) and/or AChE inhibitors [23,24]. Furthermore, there is a rapidly growing interest in coumarin derivatives in view of their marked implication in the improvement of cognitive functions of patients with neurodegenerative disease [25].

Despite the fact that the tacrine and coumarin functionalities have separately shown considerable efficacy in the treatment of Alzheimer's disease, only a limited effort was made to design tacrine-coumarin hybrids as novel multifunctional cholinesterase inhibitors. Accordingly, we have prepared a series of compounds containing both tacrine and 7-hydroxycoumarin moieties and studied their effectiveness in such roles as the ability to inhibit the enzymes acetylcholinesterase and butylcholinesterase, and the self-induced A- β aggregation process. We have also made detailed studies on these compounds in order to determine their antioxidant activity, copper-chelating properties and protective effects against the formation of free radicals (and DNA damage caused by free radicals) generated via the Fenton reaction [9]. The particular compounds consist of a tacrine unit and a 7-hydroxycoumarin moiety substituted at the 4-position, linked by alkylendiamine or alkylene polyamine tethers of different lengths via an amide functionality as shown in Fig. 1.

2. Experimental section

2.1. Chemistry: general methods and instrumentation

All solvents, chemicals, and reagents were obtained commercially and used without purification. ^1H NMR (400 MHz) and ^{13}C NMR (100 MHz) spectra were recorded on a Varian Mercury Plus NMR spectrometer using CDCl_3 or $\text{DMSO}-d_6$ as solvents with tetramethylsilane as internal standard. Chemical shifts, δ , are given in parts per million (ppm), and spin multiplicities are described as s (singlet), br s (broad singlet), d (doublet), t (triplet), q (quartet), or m (multiplet). Coupling constants, J , are expressed in hertz (Hz). Thin-layer chromatography was performed on Macherey-Nagel Alugram Sil G/UV254 plates, and spots were visualized with UV light. Chromatographic separations were performed on silica gel 60 (0.063–0.040 mm, Merck) column chromatography. Melting points were recorded on a Boetius hot-plate apparatus and are uncorrected. Yields refer to isolated pure products and were not maximized. CHN analysis was performed on a CHN analyzer PerkinElmer 2400. 2,2'-Azino-bis(3-ethylbenzothiazoline-6-sulfonic acid) diammonium salt (ABTS), potassium persulfate ($\text{K}_2\text{S}_2\text{O}_8$) and 6-hydroxy-2,5,7,8-tetramethylchroman-2-carboxylic acid (trolox) were obtained from Sigma-Aldrich (St. Louis, MO, USA). Dimethyl sulfoxide (DMSO, ACS reagent, $\geq 99.9\%$ purity) was used for radical scavenging assay and EPR experiments. $\text{CuCl}_2 \cdot 2\text{H}_2\text{O}$ was obtained from Fluka. The spin trapping agent 5,5-dimethyl-1-pyrroline *N*-oxide (DMPO; Sigma-Aldrich) was distilled prior to the application and stored at -18°C . 4-Hydroxy-2,2,6,6-tetramethylpiperidine *N*-oxyl (Tempol,

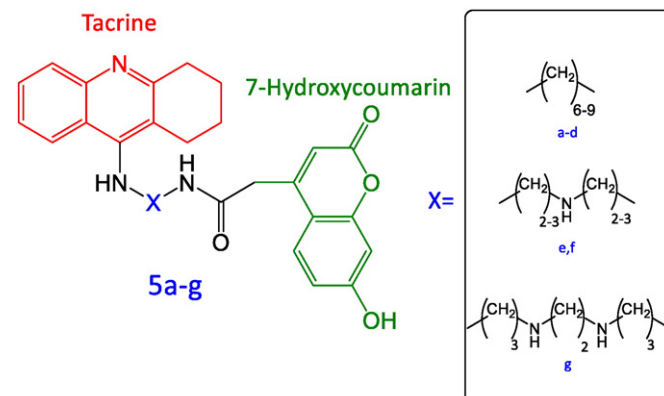


Fig. 1. Structures of tacrine, 7-hydroxycoumarin, and tacrine-coumarin hybrids 5a-g.

Sigma-Aldrich) was used as supplied. The aqueous solutions were prepared using deionized water.

The UV-vis spectra were recorded at 25 °C using a UV-3600 UV-vis-NIR spectrophotometer (Shimadzu, Japan) in a 1 cm quartz cell. A thermoelectrically temperature controlled cell holder (TCC-240A, Shimadzu) was used for controlling the temperature during measurements.

The EPR spectra of frozen solutions were measured at liquid nitrogen temperatures using a Bruker EMX series spectrometer (Karlsruhe, Germany) operating at X-band (~9.4 GHz frequency) with 100 kHz field modulation. The EPR spectrometer was interfaced with a PC dedicated for data acquisition. The g factors were determined with an uncertainty of 0.001 using an internal reference standard marker containing the stable radical 1,1-diphenyl-2-picrylhydrazyl (DPPH) built into the EPR spectrometer. For low temperature measurements cylindrical quartz sample tubes (Bruker, Karlsruhe, Germany) with 3.5 mm o.d. (ca. 3.0 mm i.d.) were used. Solid state EPR spectra were simulated using the WinEPR package (SimFonia software, Bruker, Karlsruhe, Germany) and/or software developed in our Laboratory [26]. EPR spectra of copper-drug complexes reflected axial symmetry of the systems and were interpreted using the following spin Hamiltonian [27]:

$$\hat{H} = g_{\parallel} \beta B_z \hat{S}_z + g_{\perp} \beta (B_x \hat{S}_x + B_y \hat{S}_y) + A_{\parallel} \hat{I}_z \hat{S}_z + A_{\perp} (\hat{I}_x \hat{S}_x + \hat{I}_y \hat{S}_y) \quad (2)$$

where the symbols have their usual meaning and $S = 1/2$ and $I = 3/2$ for cupric ions [28].

The EPR spectra of DMPO spin-adducts were recorded at 293 K using a EMX Plus X-band EPR spectrometer (Bruker, Germany) in a High Sensitivity Probe-head resonator (Bruker). Tacrine-coumarin hybrids 5c or 5e dissolved in DMSO were mixed with aqueous CuCl₂ and DMPO solutions, and subsequently this solution was left to stand for 15 min. To this was added H₂O₂ aqueous solution, in order to initiate the Fenton reaction. The concentration of individual reagents in the solutions was as follows (in mM): DMPO, 20; Cu(II), 0.2; tacrine-coumarin hybrid (5c or 5e) 0.2; H₂O₂, 10; the DMSO content in the mixed solvent water/DMSO represents 10% vol. In the reference experiments, the tacrine, coumarin-DMSO solution was replaced by water or DMSO. Once prepared, the solutions were carefully aerated by a gentle air stream

and the transferred immediately to a small quartz flat cell (WG 808-Q, Wilmad-LabGlass, USA). The acquisition of EPR spectra was started precisely two minutes after the hydrogen peroxide addition was made. The spin trapping experiments were carried out at least in triplicate. The concentration of spin-adducts was evaluated from the double-integrated EPR spectra, based on the calibration curve obtained from the EPR spectra of Tempol solutions measured under strictly identical experimental conditions. The experimental EPR spectra were analyzed and simulated using the Bruker software (WinEPR), and Winsim2002 software [29].

2.2. Synthesis of coumarin derivatives 3a–g and tacrine-coumarin hybrids 5a–g

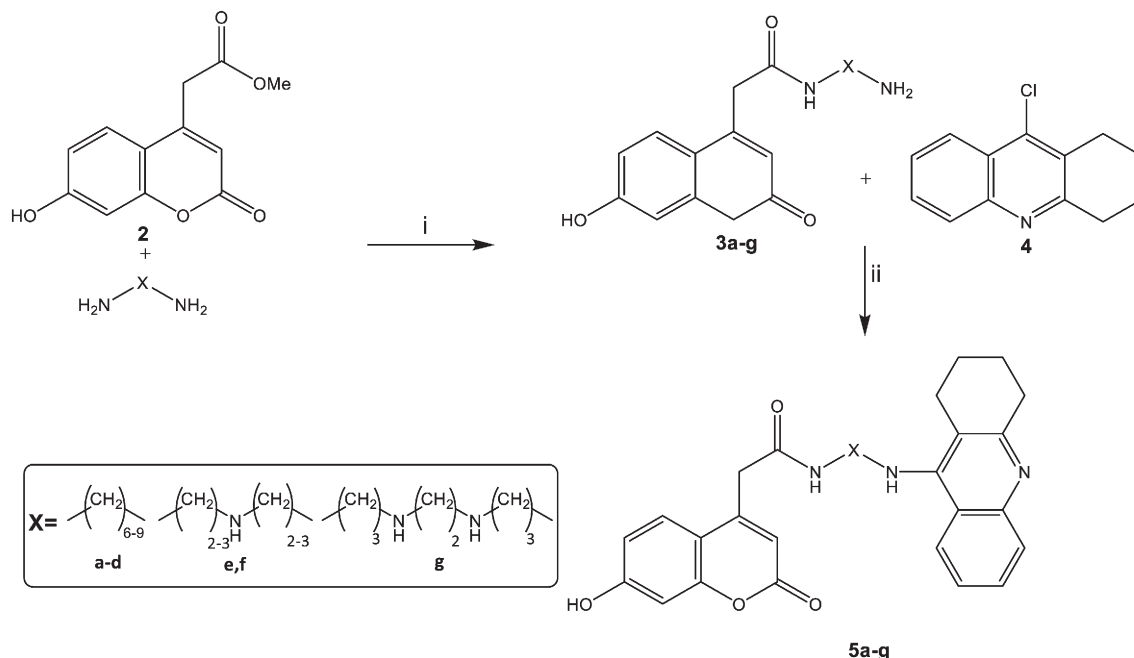
Target coumarin derivatives 3a–g and tacrine-coumarin hybrids 5a–g were synthesized as shown in Scheme 1. All of them were reported for the first time. Most of the coumarin derivatives were synthesized starting from resorcinol with citric acid in the presence of concentrated sulfuric acid [30]. Methylation of (7-hydroxy-2-oxo-2H-chromen-4-yl)acetic acid afforded the methyl ester 2 [31].

Reaction of (7-hydroxy-2-oxo-2H-chromen-4-yl)acetic acid methyl ester (2) with the relevant diamine (1,*n*-diaminoalkanes, $n = 6-9$) in acetonitrile following the reported method afforded the related acetamides 3a–g in good yields [32]. These key intermediates 3a–g then underwent reaction with 9-chloro-1,2,3,4-tetrahydroacridine (4) in the presence of phenol to provide the target tacrine-coumarin hybrids 5a–g (Scheme 1) [33].

^aReagents and conditions: (i) CH₃CN, reflux, 6 h; (ii) phenol, reflux, 6 h.

2.3. General procedure for the synthesis of *N*-1-(*n*-aminoalkyl)-2-(7-hydroxy-2-oxo-2H-chromen-4-yl)acetamides 3a–g

To a solution of the corresponding diaminoalkane (3.4 mmol) in acetonitrile (10 mL) was added (7-hydroxy-2-oxo-2H-chromen-4-yl)acetic acid methyl ester (2, 0.2 g, 0.85 mmol). The reaction mixture was stirred under reflux for 6 h. The solvent was evaporated in vacuo and the obtained residue purified by silica gel chromatography with MeOH/NH₄OH (15:1) as eluent to give compounds 3a–g as yellow



Scheme 1. Synthesis of Coumarin Derivatives 3a–g and Tacrine-Coumarin Hybrids 5a–g.^a

solid. Additional details concerning the synthesis and spectroscopic and thermal characterization of all prepared hybrids can be found in Supplementary material.

2.4. *In vitro* anti-cholinesterase assay

The AChE and BuChE inhibitory activity of the tested compounds was determined using a modified Ellman's method [34]. Human recombinant acetylcholinesterase (*hAChE*; EC 3.1.1.7, human plasma butyrylcholinesterase (*hBuChE*; EC 3.1.1.8), 5,5'-dithiobis(2-nitrobenzoic acid) (Ellman's reagent, DTNB), phosphate buffer (PB, pH 7.4), acetylthiocholine (ATC), and butyrylthiocholine (BTC), were purchased from Sigma-Aldrich (Prague, Czech Republic). For measuring purposes Nunc polystyrene 96-well microplates with flat-bottom shape (ThermoFisher Scientific, USA) were utilized. All the assays were carried out in 0.1 M $\text{KH}_2\text{PO}_4/\text{K}_2\text{HPO}_4$ buffer, pH 7.4. Enzyme solutions were prepared at activity 2.0 units/mL in 2 mL aliquots. The assay medium (100 μL) consisted of 40 μL of 0.1 M phosphate buffer (pH 7.4), 20 μL of 0.01 M DTNB, 10 μL of enzyme, and 20 μL of 0.01 M substrate (ATC iodide solution). Assay solutions with inhibitor (10⁻³–10⁻⁹ M) were preincubated for 5 min. The reaction was started by addition of 20 μL of substrate (ATC for AChE, BTC for BuChE). The enzyme activity was determined by measuring the increase in absorbance at 412 nm at 37 °C at 2 min intervals using a Multi-mode microplate reader Synergy 2 (Vermont, USA). Each concentration was assayed in triplicate. The obtained data were used to compute the percentage inhibition according to equation:

$$I = 1 - \frac{\Delta A_i}{\Delta A_0} \quad [\%] \quad (3)$$

ΔA_i indicates the absorbance change provided by cholinesterase exposed to AChE inhibitors and ΔA_0 indicates absorbance change caused by intact cholinesterase (phosphate buffer was used instead of AChE inhibitor solution). The inhibition potency of the tested compounds was expressed as IC_{50} value (the concentration of inhibitor which causes 50% cholinesterase inhibition). Calculations were performed using software Microsoft Excel (Redmont, WA, USA) and GraphPad Prism version 5.02 for Windows, GraphPad Software, San Diego, CA, USA [35].

2.5. Radical-scavenging assay

ABTS [2,2'-azino-bis(3-ethylbenzothiazoline-6-sulphonic acid)] salt was used as a source of semi-stable radical cation ($\text{ABTS}^{\bullet+}$) [36]. Solutions of $\text{ABTS}^{\bullet+}$ were prepared by dissolving 17.2 mg of ABTS and 3.3 mg of potassium persulfate ($\text{K}_2\text{S}_2\text{O}_8$) in 5 mL of deionized water. The resulting solution was left for 20 h in the dark at room temperature to complete the oxidation to the ABTS salt. Stock solutions of $\text{ABTS}^{\bullet+}$ were prepared by diluting 1 mL of oxidized ABTS solution with 60 mL of deionized water. The exact concentration of $\text{ABTS}^{\bullet+}$ was determined using UV–vis spectroscopy assuming a molar extinction coefficient of $1.5 \times 10^4 \text{ mol}^{-1} \cdot \text{dm}^3 \cdot \text{cm}^{-1}$ at 735 nm [37].

All the compounds (drugs) studied, along with copper(II) chloride, were dissolved in DMSO to achieve a final concentration of 1 mM. For the $\text{ABTS}^{\bullet+}$ scavenging study of tacrine-coumarin hybrids, 1 mM stock solutions of all compounds studied were prepared in DMSO. To study the role of copper(II) on the radical scavenging efficiency of the compounds, 1:1 copper(II)-compound complexes were prepared in DMSO and their radical-scavenging activity was studied. The kinetics of the reaction of $\text{ABTS}^{\bullet+}$ in the systems studied was monitored at a fixed wavelength of 735 nm for 15 min, which was found to be sufficient time to allow the system to reach a steady state level. The decay of $\text{ABTS}^{\bullet+}$ was monitored in the presence of 100 μL of 1 mM solutions of 5a–g in DMSO and 100 μL of DMSO placed in a 1 cm quartz cell, to which 2.8 mL of the $\text{ABTS}^{\bullet+}$ aqueous solution was added rapidly. Twelve seconds after the mixing of the solution, the absorbance change at

735 nm was monitored, or a set of UV–vis spectra in the region 260–1000 nm was measured over 900 s with a UV–vis spectrometer (UV-3600 Shimadzu, Japan). In the reference experiments, the tacrine-coumarin DMSO solution was replaced by 100 μL of DMSO. To ascertain the role of copper(II) ions on the $\text{ABTS}^{\bullet+}$ radical-scavenging activity, the same experiment was performed using 100 μL of a 1 mM DMSO solution of copper(II) chloride instead of 100 μL of DMSO. The results obtained with $\text{ABTS}^{\bullet+}$ are evaluated as trolox equivalent antioxidant capacities (TEAC) [38]. All experiments were performed in triplicate, and hence the data are representative of three independent experiments.

2.6. DNA protection assay

For the gel electrophoresis assay, plasmid DNA pBSK+ was purified using commercially available kit (Isolate II Plasmid Mini Kit, Bioline) from overnight liquid culture of *Escherichia coli* DH5 α cells grown in the LB (Luria-Bertani) medium with Ampicilin ($50 \mu\text{g} \cdot \text{mL}^{-1}$) at 37 °C for 16 h under continuous shaking (150 rpm, Heidolf Unimax 1010 incubating shaker, Germany). The DNA concentration was measured on a NanoDrop ND-1000 spectrophotometer (Nanodrop Technologies, USA). Absorbance ratios A_{260}/A_{230} determined in the range 2.0–2.2 and $A_{260}/A_{280} \geq 1.8$ indicated a sufficient purity of the DNA samples.

The compounds studied (5 μM) dissolved in DMSO were added to the 5 μM solution of CuCl_2 . The reaction mixture was allowed to stand for 15 min at room temperature (RT). Then, 15 μM of pBSK+ DNA in 50 mM sodium phosphate buffer (pH 7.2) and hydrogen peroxide was added and following their incubation (30 min at RT) the reaction mixtures were mixed with 4 μL of loading buffer (0.25% bromophenol blue in 30% glycerol). Control experiments were conducted with copper salt and hydrogen peroxide (Fenton type reaction) in the absence of the compounds added in the remaining experiments. Similar electrophoresis experiments were conducted with additional added scavenging agents (prior to addition of hydrogen peroxide), whose quantities were as follows: L-histidine (20 mM), DMSO (6 μL) and superoxide dismutase (SOD) enzyme (15U).

Samples were separated on the 0.8% agarose gel containing ethidium bromide (10 $\mu\text{mol}/\text{mL}$), in TBE buffer (89 mM Tris-borate acid, 2 mM EDTA, pH 8.0) for 1.5 h at 80 V and photographed under UV light (Kodak Gel Logic 200, Eastman Kodak Company, USA).

2.7. A- β_{1-40} amyloid fibrillization

1 mg of A- β_{1-40} powder was dissolved at 665 μM in 10 mM NaOH. The concentration was determined using UV–vis spectroscopy (Jasco V-630) with molar extinction coefficient $\epsilon_{292} = 2300 \text{ M}^{-1} \text{cm}^{-1}$. The solution was sonicated for 1 min in a bath sonicator, and centrifuged for 10 min at 12,000g at 4 °C to precipitate large aggregates. The stock solution was diluted to a final 10 μM concentration in 150 mM 3-(N-morpholino)-propanesulfonic acid (MOPS) buffer containing 0.03% NaN_3 at pH 6.9. For fibril preparation, the 10 μM A- β_{1-40} solution was incubated for 7 days at 37 °C. Fibril formation was confirmed using Thioflavin T (ThT) fluorescence assay and atomic force microscopy.

2.8. Thioflavin T assay

Binding of Thioflavin T to amyloid aggregates is characterized by an increase in its fluorescence intensity. ThT was added to A- β_{1-40} samples (10 μM) to a final concentration of 20 μM and samples were incubated at 37 °C for 1 h in the dark. The fluorescence intensity was measured using a 96-well plate by a Synergy MX (BioTek) spectrofluorimeter. The excitation was set at 440 nm and emission recorded at 485 nm. The excitation and emission slits were adjusted to 9.0/9.0 nm and the top probe vertical offset was 6 nm.

2.9. Inhibiting activity of tacrine-coumarin hybrids on A- β_{1-40} amyloid fibrillization

Tacrine-coumarin hybrids 5a–g at three different concentrations (100 pM, 10 nM and 1 μ M) were added to 10 μ M A- β_{1-40} peptide solution and the samples exposed to conditions leading to A- β_{40} peptide aggregation. The ability of the hybrids to inhibit A- β_{40} peptide fibrillization was determined using Thioflavin T assay. The experiments were performed in triplicate and the presented values are the averages of the measured values with standard deviation.

3. Results and discussion

Methods for the synthesis of coumarin derivatives and tacrine-coumarin hybrids are described in the Experimental section. In total, seven new compounds were prepared and which were grouped into two sub-groups based on the character of the linker-chain connecting the coumarin and tacrine moieties. While group one (compounds 5a–d) consists of compounds containing a linker composed of methylene groups, the linker of the second series (compounds 5e–g) is built up similarly but it additionally contains imino groups. As we show later, the nature of the spacer affects both the radical-scavenging and metal-chelating properties of the drugs. We now discuss, firstly, those results pertaining to the free radical-scavenging activity of the tacrine-coumarin hybrids.

3.1. Radical-scavenging study

Tacrine-coumarin hybrids reported in this work contain the 7-hydroxycoumarin (umbelliferone) moiety which may have protective effects against the action of free radicals [39]. Free radical scavenging activity of all studied compounds was evaluated using ABTS radical cation (ABTS $^{\bullet+}$) decolorization assay [40]. As an example, Fig. 2 shows the time-dependent changes in the UV–vis spectrum of ABTS $^{\bullet+}$ in the presence of sample 5f. The results of the scavenging capacity of the studied tacrine-coumarin hybrids as well as that of their (1:1) copper(II) complexes against the ABTS $^{\bullet+}$ are presented in Fig. 3A and B.

Fig. 3 shows the radical-scavenging effect of samples 5a–d (group 1) and their copper(II) complexes against ABTS $^{\bullet+}$. The most efficient scavenging effect against ABTS $^{\bullet+}$ was observed for sample 5c followed in sequence by samples 5a, 5b and 5d. Interaction of the drugs with copper(II) ions enhanced the radical-scavenging activity of the parent molecules. This confirms that the interaction of tacrine-coumarin hybrids with cupric ion makes their oxidation easier, as substantiated by the more profound decrease in absorption of ABTS $^{\bullet+}$. Based on these findings it may be concluded that the number of methylene units in

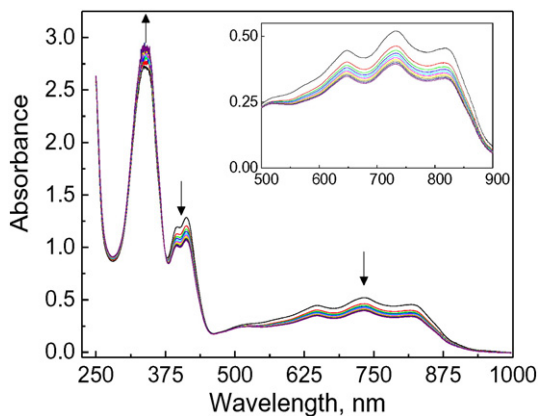


Fig. 2. Time-dependent set of electronic absorption spectra of ABTS $^{\bullet+}$ measured in the presence of drug 5f in the mixed solvent water/DMSO (DMSO content 6.7%, vol.). Inset shows the detailed decrease in the absorbance of ABTS $^{\bullet+}$ with time.

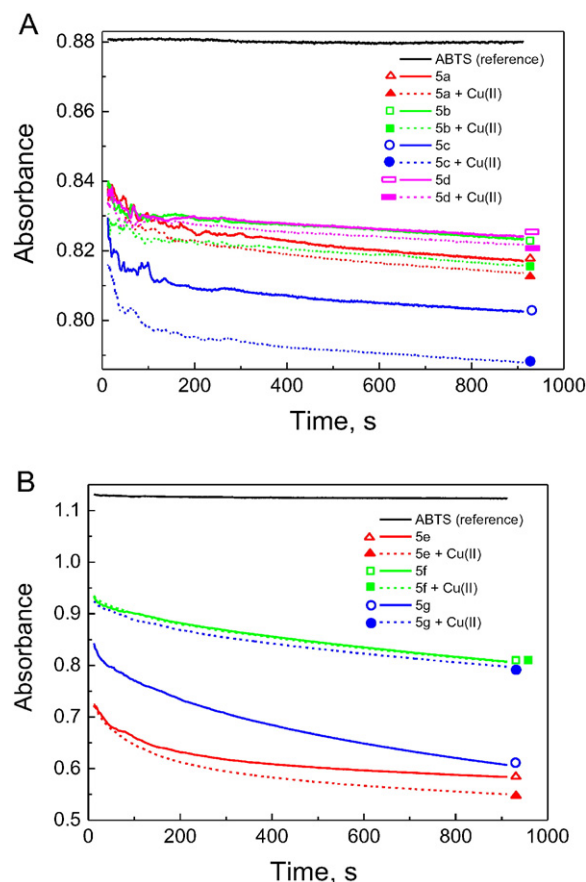


Fig. 3. Panel A. Absorbance changes of ABTS $^{\bullet+}$ at 735 nm upon time in the presence of tacrine-coumarin hybrids 5a–d in the mixed solvent water/DMSO (DMSO content 6.7%, vol.). Initial concentration of ABTS $^{\bullet+}$ was 24.5 μ M, concentration of hybrids was 0.033 mM. Radical-scavenging experiments were performed for the parent compounds as well as their (1:1) copper(II)-drug complexes. Panel B. Absorbance changes of ABTS $^{\bullet+}$ at 735 nm upon time in the presence of tacrine-coumarin hybrids 5e–g in the mixed solvent water/DMSO (DMSO content 6.7%, vol.). Initial concentration of ABTS $^{\bullet+}$ was 31.4 μ M, concentration of hybrids was 0.033 mM. Radical-scavenging experiments were performed for the parent compounds as well as their (1:1) copper(II)-drug complexes.

the spacer has a certain effect on the radical-scavenging properties of the drugs, with the optimal length being 8 methylene units.

More significant radical-scavenging activity of tacrine-coumarin hybrids against the ABTS $^{\bullet+}$ was observed for group 2 compounds 5e–g (see Fig. 3). Sample 5e exhibited the most profound radical scavenging effect followed in sequence by samples 5g and 5f. This indicates that incorporation of an additional —NH group(s) into the spacer connecting the tacrine and coumarin moieties affects the radical scavenging activity of the drugs, albeit not in an —NH number-dependent manner.

The presence of copper(II) ions on the radical scavenging activity of the group 2 compounds was not straightforward. Whereas for sample 5e the presence of copper(II) ions improved radical scavenging activity, but only slightly, sample 5f was almost unaffected by the presence of copper(II) ions, and surprisingly sample 5g in the presence of copper(II) ions exhibited even suppressed radical scavenging activity. Thus the ABTS assay confirmed that the presence of copper(II) ions has only a mild effect on the radical scavenging activity of the group 2 samples.

As already noted above, the tacrine-coumarin hybrids presented in this study contain residues of 1,2,3,4-tetrahydroacridine and 7-hydroxycoumarin. The radical-scavenging activity of the drugs presented in this study can be attributed only to the presence of the 7-OH-group of 7-hydroxy coumarin and the —NH groups in the spacer connecting the tacrine and coumarin moieties. Generally, incorporation of —NH groups into the spacer increased radical-scavenging activity, as

documented by the radical scavenging experiments in the group 2 samples (5e–g). The results obtained with ABTS^{•+} for all the studied substances are evaluated as trolox equivalent antioxidant capacities (TEAC) [38] and are presented in Table 1. It is evident that group 2 (compounds 5e–g) demonstrates potentially important antioxidant power which may attenuate the oxidative stress component typical for AD.

3.2. Copper(II) complexation with hybrids 5a–g

Electron paramagnetic resonance spectroscopy (EPR) is a physical technique sensitive to the immediate environment around a paramagnetic centre, and hence it can be conveniently employed to elucidate the binding mode between copper(II) ion and drugs [41]. Since copper was introduced into the studied system in the form of copper(II) chloride and the aim was to see the effect of the coordinated drug, a control EPR experiment was performed with copper(II) chloride in the absence of the drug. The EPR spectrum of CuCl₂·2H₂O in DMSO at 77 K is shown in Fig. 4. The spectrum indicates that the copper(II) ion coordinated by DMSO molecules is of nearly axial symmetry (a weak rhombic splitting is seen) with all four hyperfine splitting bands well resolved in the parallel region. Hyperfine splitting in the perpendicular region of the spectrum was not observed. The low-temperature EPR spectra of copper(II)-drug complexes are presented in Fig. 4. At first sight the EPR spectra of Cu(II)-drug complexes appear to be similar to the spectrum of copper(II) chloride in the absence of drug. All of the observed EPR spectra exhibit high values of $g_{||}$ and relatively low values of $A_{||}$ indicating marked tetrahedral distortion around copper(II) ion substantiated by the quotient $g_{||}/A_{||}$ (~220 cm) which has been introduced as a convenient measure of the degree of tetrahedral distortion [42].

The shape of the EPR spectrum is dependent on the nature of the ligands directly coordinated to the metal ion as well as on the stereochemical arrangement of ligands around the metal ion [41]. If the coordinated atom has a non-zero nuclear spin (for example ¹⁴N, $I = 1$), the interaction of the nuclear spin of the ligand with an unpaired electron on the metal ion leads to a splitting (often termed as superhyperfine splitting) of spectral lines [28]. Although such splitting often cannot be resolved, metal complexes with directly bonded magnetically active nitrogens (the naturally abundant isotope ¹⁶O has zero nuclear spin and does not contribute to hyperfine splitting) exhibit somewhat broader EPR hyperfine lines [42]. Thus metal ions coordinated exclusively with oxygen donor ligands may have narrower EPR lines.

A detailed inspection of the low-field parallel lines ($m_l = -3/2$) in the studied systems revealed that in contrast to the rather narrow line observed for copper chloride, a slightly broader $m_l = -3/2$ line was observed for the copper(II)-drug complexes [42]. A similar trend was observed also for lines corresponding to higher quantum numbers. Thus in spite of the similarity in the EPR spectra of copper chloride and copper-drugs it may be concluded that interaction between the copper ion and drug has occurred, most probably involving amido-nitrogen and carbonyl oxygen of the spacer (see Fig. 5). The remaining binding positions around the copper ion may be occupied by solvent molecules. Metal-drug interaction was indirectly confirmed by UV–vis

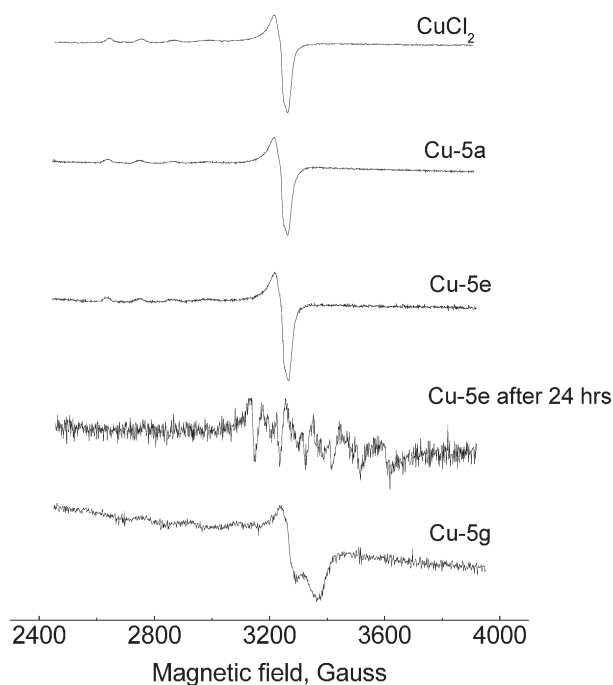


Fig. 4. EPR spectra of copper(II) chloride (1 mM) and (1:1) copper(II) complexes with tacrine-coumarin hybrids 5a, 5e and 5g (1 mM) in DMSO at 77 K. Residual EPR signal for 5e after 24 h corresponds to the manganese impurities originating from the starting compounds.

spectroscopy which revealed altered (mostly enhanced) radical scavenging activity of the drugs in the presence of copper(II) ions.

The EPR spectra of some of the Cu(II)-drug complexes have been found to be time-dependent. A gradual time-dependent decrease in EPR spectral intensity has been observed 15 min after preparation of the copper(II) complexes of compounds 5e–g. The EPR spectra of complexes 5a–d did not exhibit any significant change in spectral intensity with time. The EPR spectra of copper(II) complexes were re-measured 24 h after their preparation and confirmed the results obtained after 15 min. The time dependent changes of the EPR spectra for Cu(II) complexes with compounds 5e–g indicate that the loss of EPR signal

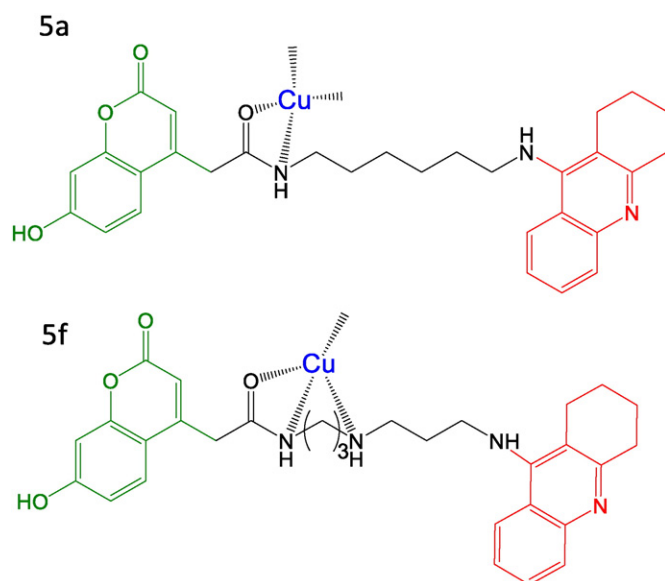


Fig. 5. Schematic drawings of copper(II) binding to compounds 5a–d (drug 5a) and compounds 5e–g (drug 5f) tacrine-coumarin hybrids.

Table 1
The results of ABTS^{•+} assay for compounds 5a–g and their (1:1) copper(II) complexes.

Compound	TEAC ^a	(1:1) copper complexes	TEAC
5a	0.06	Cu-5a	0.07
5b	0.05	Cu-5b	0.07
5c	0.08	Cu-5c	0.09
5d	0.06	Cu-5d	0.06
5e	0.54	Cu-5e	0.57
5f	0.32	Cu-5f	0.32
5g	0.52	Cu-5g	0.33

^a The results are expressed as Trolox equivalent antioxidant capacity (TEAC).

intensity is accompanied by a conversion of paramagnetic cupric ions to diamagnetic (EPR silent) cuprous species. This indicates that the —NH groups in the spacer connecting the tacrine and coumarin moieties in 5e–g are involved in the binding to copper(II) ions (Fig. 5).

3.3. EPR spin trapping study

As discussed above, certain redox metals, including copper ions, are efficient catalysts for the decomposition of hydrogen peroxide via the Fenton reaction (Eq. 1) [9]. The catalytic activity of a redox metal ion is partly dependent on the ligand environment around the metal centre. Since the maximal coordination number of a copper ion is six, a hexadentate-ligand (chelator) can result in metal-complexes that are catalytically inert because the coordination sphere of the copper ion is completely saturated, and hence it is not possible to bind a further molecule for catalytic transformation [43]. In order to ascertain the protective effect of the compounds studied (which possess metal chelating properties) in the copper catalyzed decomposition of hydrogen peroxide to hydroxyl radicals, a series of EPR spin trapping experiments was performed, which consisted of a study of two reactions. In the reference reaction, free copper ions (introduced into the system in the form of copper(II) chloride) were used to catalyse the decomposition of hydrogen peroxide to yield hydroxyl radicals which were trapped by the DMPO spin trap in the form of $\cdot\text{DMPO-OH}$ spin-adducts, under the given experimental conditions. To determine the effect of samples 5c and 5e on the formation of hydroxyl radicals, the copper ions were introduced into the reaction mixture in the form of (1:1) copper(II)-5c or (1:1) copper(II)-5e complexes. In this case, similarly to the reference system, the copper(II)-complexes catalyzed the decomposition of hydrogen peroxide with the formation of hydroxyl radicals (Fenton reaction) which were trapped by DMPO to yield $\cdot\text{DMPO-OH}$ spin-adduct radicals [44]. The intensity of the EPR signal from $\cdot\text{DMPO-OH}$ for systems containing copper(II) complexes with 5e or 5c was reduced from that measured in the reference reaction system (spectra not shown). Since the double-integrated intensity of the EPR spectrum is directly proportional to the concentration of radicals in the sample, the concentration of spin-adducts was evaluated from the double-integrated EPR spectra of $\cdot\text{DMPO-OH}$ spin-adducts. Specific spin-adduct concentrations were determined from the calibration curve obtained from the EPR spectra of Tempol solutions measured under strictly identical experimental conditions. The corresponding results are presented in Fig. 6,

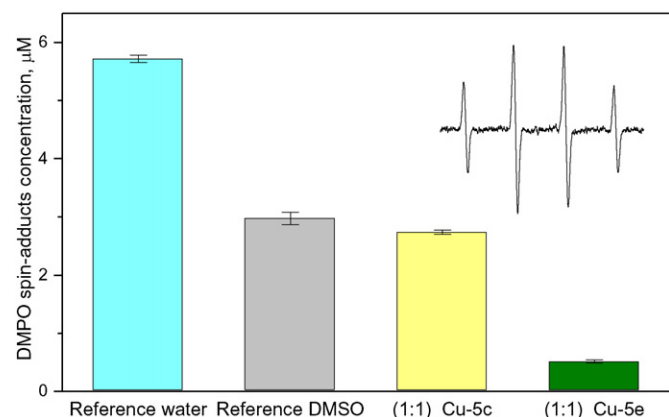


Fig. 6. Concentrations of $\cdot\text{DMPO-OH}$ spin-adducts monitored in the following Fenton-like systems: ■ reference system containing copper(II), hydrogen peroxide and DMPO spin trap in water; ■ reference system containing copper(II), hydrogen peroxide and DMPO spin trap in water/DMSO mixed solvent; ■ system containing (1:1) copper(II)-5c complex, hydrogen peroxide and DMPO spin trap in water/DMSO mixed solvent; ■ system containing (1:1) copper(II)-5e complex, hydrogen peroxide and DMPO spin trap in water/DMSO mixed solvent. DMSO content in the mixed solvent was 6.7% vol. Inset shows the EPR spectrum of $\cdot\text{DMPO-OH}$ spin-adduct ($a_N = 1.496$ mT, $a_H = 1.455$ mT; $g = 2.0058$).

which show that while the introduction of 5c to the system causes an only minor reduction in the $\cdot\text{DMPO-OH}$ spin-adduct concentration, the presence of the compound 5e brings about a profound decrease in the level of radical production. This suggests that chelation of copper(II) ions by compound 5e provides a marked protection against the copper-catalyzed formation of reactive hydroxyl radicals, and is of particular significance because coordination of 5e to cupric ions resulted in their reduction to cuprous species (discussed above) which are known to act as highly effective catalysts in the Fenton reaction [43]. Thus, we may consider that there are two opposing effects which operate when the compound 5e becomes coordinated to copper(II) ions. On the one hand, chelation of copper(II) by 5e results in the formation of a catalytically inert copper-5e complex with a saturated coordination environment around the metal ion, and an accordingly suppressed catalytic activity, hence a decreased formation of hydroxyl radicals via the Fenton reaction. However, within that saturated coordination environment around the copper ions, reduction of copper(II) by 5e results in the conversion of cupric into cuprous ions, so to form a Cu(I)-5e complex which is catalytically active in the Fenton reaction. On the basis of the results obtained (Fig. 6), we may deduce that the influence of copper-chelation is stronger than that of copper-reduction for 5e, in view of the profoundly reduced quantity of hydroxyl radicals generated via the Fenton reaction, as compared with the control (reference) experiment. This promising protective effect of the drug 5e in the suppression of copper-induced oxidative stress in Alzheimer's disease was further assessed by in vitro DNA damage experiments.

3.4. DNA protection study

Plasmid DNA, which occurs mainly in closed circular form (SC, supercoiled form), can be cleaved either in the presence of intercalating molecules and/or in the presence of reactive radical species. The DNA cleavage leads to the formation of new conformational states of the plasmid molecule (linear and nicked form) which may be discerned in agarose gels as bands with decreased mobility, the intensity of which may be used to assess relative degrees of DNA damage. Thus, the gel-electrophoresis method provides an effective means to determine whether a particular substance causes a disruption of the DNA structure (by functioning as a chemical nuclease) [45,46] or protects it via a radical scavenging mechanism, and/or chelation of redox active metal ions (by functioning as an antioxidant) [47,48].

Selected compounds (5c, 5e) dissolved in DMSO were studied using gel-electrophoresis for their ability to reduce DNA damage following reaction with pBSK + plasmid under Fenton-conditions (in the presence of Cu(II) ions and H_2O_2), (Fig. 7, Line 1a, 1b). Plasmid DNA was exposed to a 5 μM concentration of each of the compounds 5c and 5e, in the presence of an equimolar concentration of copper and a 250-fold higher concentration of hydrogen peroxide. To detect which active oxygen species are formed in the reaction mixture and whether the substances under study can contribute to radical scavenging, the experiments were performed in the presence of separately added scavenging agents such as L-histidine, DMSO and SOD enzyme, for scavenging singlet oxygen, hydroxyl radical and superoxide anion radical, respectively (Fig. 7, Line 2–4, 2a–4a, 2b–4b). Control experiments were carried out in the absence of either compound (Fig. 7, Line 1–4).

The electrophoretic profile shows, as expected, a loss of the signal from the supercoiled form of DNA, and the formation of the nicked DNA form, in the presence of copper and hydrogen peroxide (Fig. 7, Line 1) as a result of damage to DNA by reactive radicals. The more intense signal from the supercoiled form of plasmid DNA, observed following the introduction of respective scavenging agents into the reaction mixture (Lane 2–4), indicates that singlet oxygen ($^1\text{O}_2$) (Line 2), hydroxyl radicals ($\cdot\text{OH}$) (Line 3) and superoxide anion radicals ($\text{O}_2^{\cdot-}$) (Line 4) are the reactive species which participate in the cleavage of DNA [48]. The formation of singlet oxygen ($^1\text{O}_2$) can be explained on the basis of the protonated form of the superoxide radical [termed

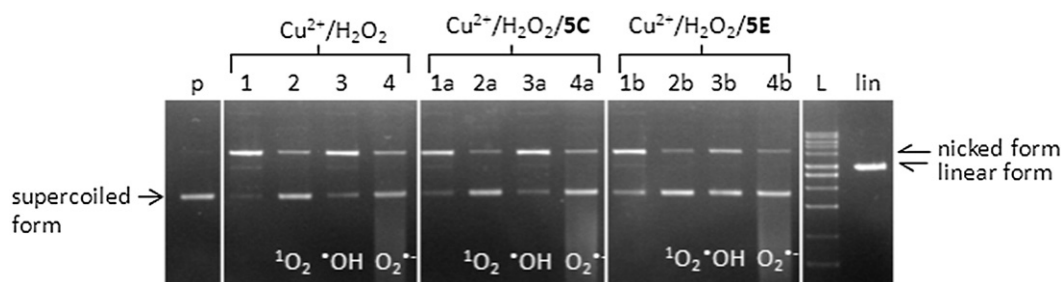


Fig. 7. Agarose gel (0.8%) showing the behaviour of compounds 5c, 5e (5 μM) under in vitro conditions of Fenton type reaction (5 μM CuCl_2 + 250 μM H_2O_2), and after addition of radical scavengers. All reaction mixtures occupied a final volume of 15 μL . Lanes represent: (p) control plasmid DNA, (1) plasmid + CuCl_2 + H_2O_2 ; (2) plasmid + CuCl_2 + H_2O_2 + L-his (20 mM); (3) plasmid + CuCl_2 + H_2O_2 + DMSO (6 μL); (4) plasmid + CuCl_2 + H_2O_2 + SOD (15 U); (1a–4a) same as lanes 1–4 with adding compound 5c; (1b–4b) same as lanes 1–4 with adding compound 5e; (L) 1 kb DNA ladder, (lin) plasmid linearized with EcoRI endonuclease (as a control for double strand cleavage). Individual compounds 5c or 5e did not show any signs of interaction with DNA (data not shown).

the hydroperoxyl radical or perhydroxyl radical ($\cdot\text{OOH}$), which can undergo a combination step, followed by collapse of the tetroxide intermediate (Eq. 4) [49]



Based on the signal from the supercoiled DNA form, we could observe that DNA damage is diminished when the substances 5c (Line 1a) and 5e (Line 1b) are present in the mixture, as compared with the control experiment (Line 1). The slightly more intense signal of supercoiled DNA (Line 1b) allows us to suppose that the substance 5e has a stronger protective effect than the substance 5c (Line 1a). The results from the reactions performed in the presence of radical scavengers showed that the compound 5e contributes toward the greatest DNA protection, mainly by the mechanism of hydroxyl radical scavenging. This is supported by a stronger signal from supercoiled DNA being observed following the addition of DMSO (Line 3b). Based on the signal attenuation of the nicked DNA form, when SOD enzyme is present (Line 4b), some contribution to the overall DNA protection may also be attributed to scavenging of the superoxide anion radical [46]. An analysis of the electrophoregrams has also shown that both substances can partially scavenge singlet oxygen (Line 2a, 2b), as deduced in the gel from a weaker signal of the nicked DNA form. Overall, these results indicate that compound 5e has the greatest antioxidant potential.

3.5. Inhibition of human AChE and BuChE

The anticholinesterase activity of newly synthesized hybrids 5a–g was evaluated. The inhibitory activity was expressed as the concentration at which 50% of enzyme activity was inhibited (IC_{50}). The IC_{50} values of compounds 5a–g were determined against human erythrocyte AChE (*hAChE*, E.C. 3.1.1.7) and against human plasmatic butyrylcholinesterase (*hBuChE*, E.C. 3.1.1.8) using the method of Ellman et al [34]. The

Table 2

In vitro inhibition of human cholinesterases (*hAChE* and *hBuChE*) by tacrine-coumarin hybrids 5a–g and control compounds tacrine and 7-MEOTA.

Compounds	X	IC_{50} (nM) ^a <i>hAChE</i>	IC_{50} (nM) ^b <i>hBuChE</i>
5a	(CH ₂) ₆	65.6 ± 2.3	103.8 ± 3.4
5b	(CH ₂) ₇	71.8 ± 1.5	63.5 ± 1.3
5c	(CH ₂) ₈	79.2 ± 1.8	71.9 ± 1.1
5d	(CH ₂) ₉	120.7 ± 6.1	84.2 ± 0.8
5e	(CH ₂) ₂ -NH-(CH ₂) ₂	51.4 ± 1.9	676.2 ± 22.8
5f	(CH ₂) ₃ -NH-(CH ₂) ₃	49.9 ± 1.4	103.8 ± 3.1
5g	(CH ₂) ₃ -NH-(CH ₂) ₂ -NH-(CH ₂) ₃	38.3 ± 1.3	168.4 ± 5.0
Tacrine		500 ± 100	23 ± 4
7-MEOTA		15,000 ± 2900	21,000 ± 3400

^a IC_{50} : inhibitory concentration of AChE.

^b IC_{50} : inhibitory concentration of BuChE.

IC_{50} values of tacrine-coumarin hybrids 5a–g and the control compounds tacrine and 7-MEOTA [50] are summarized in Table 2.

The IC_{50} values suggested that most of the designed tacrine-coumarin hybrids 5a–g exhibited potent and selective inhibitory activities in the nanomolar range toward both *hAChE* and *hBuChE*, being in general more potent than the reference compounds tacrine and 7-MEOTA. Amongst the target compounds, 5g (IC_{50} = 38.3 nM) showed the highest inhibitory activity against AChE, and the potency was 13- and 392-times stronger than that of the reference compounds tacrine (IC_{50} = 500 nM) and 7-MEOTA (IC_{50} = 15,000 nM), respectively. Compound 5b exhibited the strongest inhibition against BuChE with a value of 63.5 nM, which was 330-fold more potent than that of 7-MEOTA (IC_{50} = 21,000 nM). The linker length between the coumarin moiety and the tetrahydroacridine skeleton played a significant role in determining the inhibitory activity for AChE. Tacrine-coumarin hybrids 5a–d showed decreasing AChE inhibitory activity with increasing length of the alkyl chain spacer from six to nine carbon atoms. Conversely, for compounds 5e–g containing additional secondary amine group(s) in the spacer, an increasing number of methylene and amino groups resulted in an increase in AChE activity [51]. This suggested that the shortest six-carbon linker (derivative 5a) and the longest carbon/nitrogen linker (derivative 5g) are the most promising AChE inhibitors. The obtained data indicate that these linkers allow optimal interaction between the aromatic moieties of the inhibitors and the CAS and PAS of the enzymes. No correlation between the length/nature of the spacer and BuChE inhibitory activity was observed for 5a–g. The alkyl chain with seven-carbon linker between two amino groups (derivative 5b) seemed to be most beneficial for BuChE activity.

3.6. Kinetic analysis of the AChE inhibition

The mechanism involved in AChE inhibition was investigated using the two most potent cholinesterase inhibitors 5g (IC_{50} = 38.3 ± 1.3 nM for AChE) and 5b (IC_{50} = 63.5 ± 1.3 nM for BuChE). The type of inhibition was elucidated from nonlinear regression analysis. Results for each type of inhibition model (competitive, noncompetitive, uncompetitive and mixed) were compared with the sum-of-squares *F*-test. Analysis confirmed a mixed type of inhibition ($p < 0.05$) for both compounds. With increasing concentration of inhibitor the apparent V_{max} decreased and K_m increased, due to binding to both free and substrate-bound enzyme. Fig. 8 shows Lineweaver-Burk reciprocal plots of observed data. K_i values of 61.6 ± 1.4 nM for 5g and 17.0 ± 0.4 nM for 5b were estimated by nonlinear regression analysis.

3.7. Inhibition of A- β _{1–40} amyloid aggregation

One of the main hallmarks of AD is the presence of amyloid plaques composed of A- β amyloid aggregates. We were interested to ascertain using Thioflavin T assay if the studied tacrine-coumarin hybrids are able to inhibit formation of A- β _{1–40} amyloid fibrils. Thioflavin T is a

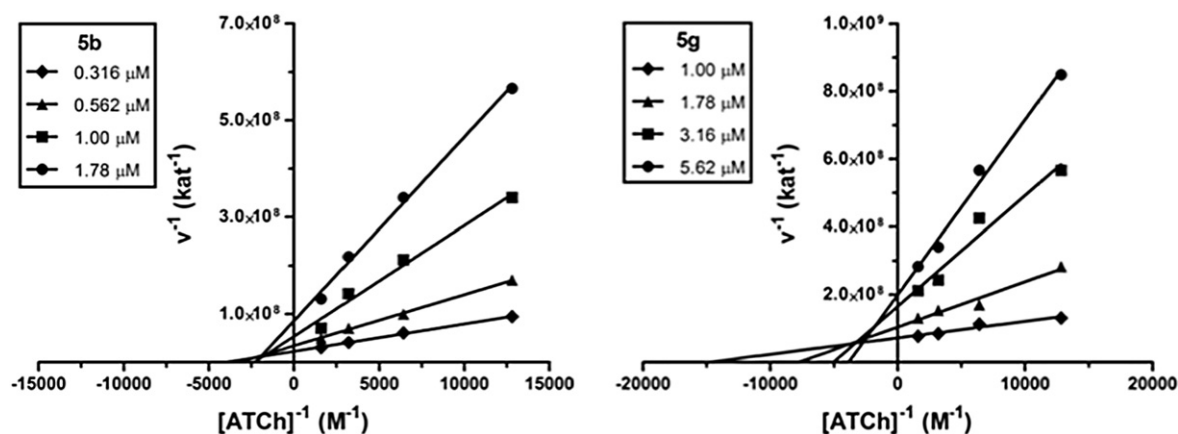


Fig. 8. Steady-state inhibition of AChE hydrolysis of acetylthiocholine (ATCh) by compounds 5b and 5g. Lineweaver-Burk reciprocal plots of initial velocity and different substrate concentrations (0.78–6.25 mM) are presented. Lines were derived from a weighted least-squares analysis of data.

specific fluorescent dye which shows significant increase in its fluorescence intensity upon binding to amyloid fibrils [52]. The results obtained for three different compound concentrations (100 pM, 10 nM and 1 μM) and 10 μM A-β_{1–40} peptide are presented in Fig. 9. The data were normalized to the fluorescence intensity detected for untreated A-β_{1–40} amyloid fibrillization. For low concentrations of tacrine-coumarin hybrids (100 pM and 10 nM) the obtained data show no significant changes in fluorescence intensities compare to the intensity of A-β_{1–40} alone. However, the highest concentration (1 μM) of tacrine-coumarin hybrids caused a large decrease in fluorescence intensities. Based on the fluorescence data, the inhibiting activities A_{inh} were calculated and are presented in Table 3. Inhibiting activity is a measure of the ability of the studied compound to inhibit A-β₄₀ amyloid self-assembly.

The A_{inh} values were obtained as the difference in fluorescence intensity of amyloid aggregates (taken as 100%) and the normalized fluorescence detected after treatment with the compound. The data obtained at 1 μM concentration of hybrids strongly suggest that the most effective is hybrid 5c with inhibiting activity A_{inh} of about 82%. Very intensive inhibition was detected also for 5b, 5d, 5e and 5g compounds (from 65% to 58%). The lowest inhibitory activity was detected for hybrids 5a and 5f since they have only 30% inhibiting activity A_{inh} .

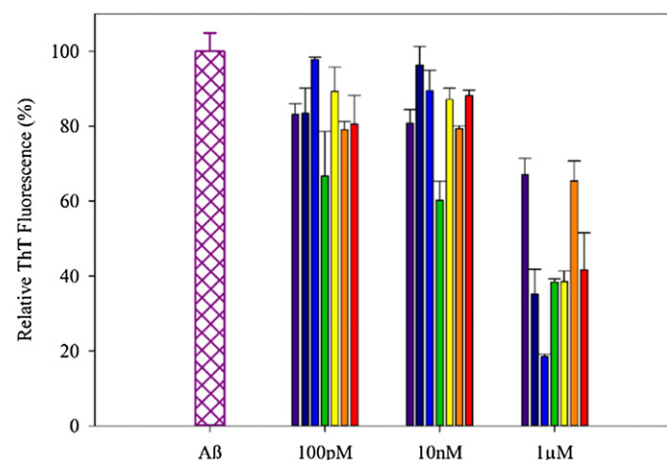


Fig. 9. ThT fluorescence intensities for A-β_{1–40} amyloid fibrils alone and in the presence of 3 different concentrations (100 pM, 10 nM and 1 μM) of tacrine-coumarin hybrids 5a–g (5a-purple, 5b-dark blue, 5c-blue, 5d-green, 5e-yellow, 5f-orange, 5g-red). The fluorescence signal for each sample was normalized to the fluorescence intensity of A-β_{1–40} amyloid fibrils alone (white bar; taken as 100%). Each experiment was performed in triplicate – colored bars represent the average, and the error bars represent standard deviation.

The obtained results suggest that in the presence of the hybrids there is a decline in amyloid A-β₄₀ fibrillization. The extent of inhibition is affected by the property of the linker. The most effective was hybrid 5c with spacer comprising a simple alkyl chain with eight carbon linker. About 20% less inhibition was observed for compounds 5b and 5d with linkers containing one carbon more or less. The incorporation of NH groups into the linker does not improve inhibition performance compared with the simpler hybrids 5a–5d. The ability of compounds 5e and 5g to inhibit fibrillization was similar to the activity detected for compounds 5b and 5d. In the case of hybrid 5f the inhibition was comparable to the activity detected for hybrid 5a. The obtained data indicate that the compound with linker comprising an eight-carbon alkyl chain represents the most effective inhibitor of A-β_{1–40} peptide aggregation.

4. Conclusions

In the present work, a series of tacrine-coumarin hybrids was designed, synthesized and evaluated for their potential use novel radical-scavengers, copper-chelators and multifunctional cholinesterase inhibitors.

The radical scavenging efficiency of all the drugs and their complexes with copper ions was studied using the ABTS^{•+} assay. In addition, complexation of the drugs with copper ions was monitored using EPR spectroscopy. According to the ABTS assay, compound 5e has the most profound radical scavenging effect. It was found that the interaction of the tacrine-coumarin hybrids with copper ions slightly enhanced their radical scavenging activity. Results from EPR spectroscopy suggested that the carbonyl oxygen and imino nitrogen atoms of the spacer were coordinated to the copper(II) ion, and confirmed the reduction of Cu(II) to Cu(I) for compounds 5e–g, which may have a number of different consequences. On the one hand, cuprous species are effective

Table 3
The inhibiting activity A_{inh} of tacrine-coumarin hybrids 5a–g.

Compound	Inhibitory activity A_{inh} ^a (%)	
	10 nM ^b	1 μM ^b
5a	19.3 ± 3.7	33.0 ± 4.4
5b	3.7 ± 5.0	64.8 ± 6.6
5c	10.5 ± 5.4	81.5 ± 0.7
5d	39.8 ± 5.1	61.6 ± 0.9
5e	12.9 ± 3.0	61.5 ± 2.9
5f	20.7 ± 0.8	34.6 ± 5.3
5g	11.9 ± 1.5	58.3 ± 9.8

^a Calculated as difference of the fluorescence intensity obtained for amyloid aggregates (taken as 100%) and normalized fluorescence detected after treatment with the compound. Fluorescence measurements were obtained by ThT assay.

^b Compound concentration. Concentration of A-β_{1–40} was 10 μM.

catalysts for generating free radicals by a Fenton-like reaction ($\text{Cu(I)} + \text{H}_2\text{O}_2 \rightarrow \text{Cu(II)} + \text{OH}^- + \bullet\text{OH}$), but on the other hand, tight copper-chelation by hybrid ligands insulates the metal ions from being catalytically active. Based on quantitative EPR spin trapping experiments, it was concluded that chelation of free copper(II) ions (known to occur in increased amounts in amyloid plaques) by tacrine-coumarin hybrids (hybrids 5c and 5e) suppresses the formation of reactive hydroxyl radicals which in turn may alleviate oxidative stress products as are typical for Alzheimer's disease. This conclusion, which corroborates a protective effect of tacrine-coumarin hybrids under conditions of copper-induced oxidative stress was further confirmed by in vitro DNA damage protection experiments. While hybrid 5c coordinated in the complex Cu-5c provided only mild protection against copper-catalyzed DNA damage via the Fenton reaction, hybrid 5e upon coordination to copper ion (complex Cu-5e) suppressed copper-catalyzed DNA damage significantly. From a quantitative point of view, the protective effect of ligands 5c and 5e in DNA damage protection experiments was found to follow the same trend as was observed from the EPR spin trapping experiments.

Most of the studied compounds inhibit *hAChE/hBuChE* at nanomolar concentrations. Compound 5g especially showed the most potent AChE inhibitory activity, which was respectively 13- and 392-fold greater than that of the reference compounds tacrine and 7-MEOTA. Kinetic study of AChE inhibition confirmed a mixed type of inhibition for compounds 5b and 5g.

The results observed using Thioflavin T assay showed that tacrine-coumarin hybrids are also able to interfere with $\text{A-}\beta_{1-40}$ aggregation in a concentration-dependent manner. In the inhibition of $\text{A-}\beta$ aggregation assay, compound 5c containing an eight-carbon alkyl chain possessed the highest inhibitory activity, as well as the most efficient scavenging effect against $\text{ABTS}^{\bullet+}$.

We may conclude that an exploration of the concept to develop drugs with which to target multiple etiologies, including the relatively scarcely studied oxidative stress component in Alzheimer's disease is a challenging task, that will require a determined effort to fulfill.

Abbreviations

AD	Alzheimer's disease
AChE	acetylcholinesterase
ACh	acetylcholine
AChEIs	acetylcholinesterase inhibitors
NMDAR	<i>N</i> -methyl-D-aspartate receptor
PAS	peripheral anionic site
CAS	catalytic anionic site
A- β	β -amyloid peptide
BuChE	butyrylcholinesterase
<i>hAChE</i>	human acetylcholinesterase
<i>hBuChE</i>	human butyrylcholinesterase
IC ₅₀	50% inhibitory concentration
EPR	electron paramagnetic resonance
ATC	acetylthiocholine
BTC	butyrylthiocholine
SOD	superoxide dismutase
ABTS	2,2'-Azino-bis(3-ethylbenzothiazoline-6-sulfonic acid) diammonium salt
PB	phosphate buffer

Acknowledgements

We would like to thank to Ms. Anna Horova for skilfull technical assistance. This work was also supported by and by the project NV15-30954A of the AZV CR, MH CZ – DRO (UHHK, 00179906), by Long Term Development Plan – 1011 of Faculty of Military Health Sciences, University of Defence and the Slovak Grant Agency VEGA (Grant 2/0181/13, 1/0765/14, 1/0041/15), APVV-0171-10, APVV-15-0079 and

ESF 26220220005. The authors are grateful to Ian McColl BSc, MD, PhD for assistance with the manuscript.

Appendix A. Supplementary data

Supplementary data to this article can be found online at <http://dx.doi.org/10.1016/j.jinorgbio.2016.05.001>.

References

- [1] D.J. Selkoe, *Science* 337 (2012) 1488–1492.
- [2] D. Munoz-Torrero, *Curr. Med. Chem.* 15 (2008) 2433–2455.
- [3] H.H. Feldman, C. Jacova, *Nature Clin. Pract. Neurol.* 5 (2009) 128–129.
- [4] E. Nepovimova, J. Korabecny, R. Dolezal, K. Babkova, A. Ondrejcek, D. Jun, V. Sepsova, A. Horova, M. Hrabina, O. Soukup, N. Bukum, P. Jost, L. Muckova, J. Kassa, D. Malinak, M. Andrs, K. Kuca, *J. Med. Chem.* 58 (2015) 8985–9003.
- [5] J. Korabecny, R. Dolezal, P. Cabelova, A. Horova, E. Hruha, J. Ricny, L. Sedlacek, E. Nepovimova, K. Spilovska, M. Andrs, K. Musilek, V. Opletalova, V. Sepsova, D. Ripova, K. Kuca, *Eur. J. Med. Chem.* 82 (2014) 426–438.
- [6] H. Oh, J. Steffener, Q.R. Razlighi, C. Habeck, Y. Stern, *J. Neurosci.* 36 (2016) 1962–1970.
- [7] M. Mamelak, *Neurobiol. Aging* 28 (2007) 1340–1360.
- [8] R. Rajendran, R. Minqin, M.D. Ynsa, G. Casadesus, M.A. Smith, G. Perry, B. Halliwell, F. Watt, *Biochem. Biophys. Res. Commun.* 382 (2009) 91–95.
- [9] M. Valko, K. Jomova, C.J. Rhodes, K. Kuca, K. Musilek, *Arch. Toxicol.* 90 (2016) 1–37.
- [10] Z. Zhu, R.J. Castellani, P.I. Moreira, G. Aliev, J.C. Shenk, S.L. Siedlak, P.L. Harris, H. Fujioka, L.M. Sayre, P.A. Szewda, L.I. Szewda, M.A. Smith, G. Perry, *Free Radic. Biol. Med.* 52 (2012) 699–704.
- [11] S. Varadarajan, S. Yatin, M. Aksenova, D.A. Butterfield, *J. Struct. Biol.* 130 (2000) 184–208.
- [12] S.S. Xie, J.S. Lan, X.B. Wang, N. Jiang, G. Dong, Z.R. Li, K.D. Wang, P.P. Guo, L.Y. Kong, *Eur. J. Med. Chem.* 93 (2015) 42–50.
- [13] E. Nepovimova, J. Korabecny, R. Dolezal, K. Babkova, A. Ondrejcek, D. Jun, V. Sepsova, A. Horova, M. Hrabina, O. Soukup, N. Bukum, P. Jost, L. Muckova, J. Kassa, D. Malinak, M. Andrs, K. Kuca, *J. Med. Chem.* 58 (2015) 8985–9003.
- [14] S. Thirathmatrakul, C. Yenjai, P. Waiwut, O. Vajragupta, P. Reubroycharoen, M. Tohda, C. Boonyarat, *Eur. J. Med. Chem.* 75 (2014) 21–30.
- [15] B. Sandhya, D. Giles, V. Mathew, G. Basavarajaswamy, R. Abraham, *Eur. J. Med. Chem.* 46 (2011) 4696–4701.
- [16] K.C. Fylaktakidou, D.J. Hadjipavlou-Litina, K.E. Litinas, D.N. Nicolaides, *Curr. Pharm. Des.* 10 (2004) 3813–3833.
- [17] M. Ghate, D. Manohar, V. Kulkarni, R.S. Shobha, Y. Kattimani, *Eur. J. Med. Chem.* 38 (2003) 297–302.
- [18] D. Vina, M.J. Matos, M. Yanez, L. Santana, E. Uriarte, *Med. Chem. Commun.* 3 (2012) 213–218.
- [19] P. Anand, B. Singh, N. Singh, *Bioorg. Med. Chem.* 20 (2012) 1175–1180.
- [20] H.C. Lin, S.H. Tsai, C.S. Chen, Y.C. Chang, C.M. Lee, Z.Y. Lai, C.M. Lin, *Biochem. Pharmacol.* 75 (2008) 1416–1425.
- [21] I. Kostova, S. Bhatia, P. Grigorov, S. Balkansky, V.S. Parmar, A.K. Prasad, L. Saso, *Curr. Med. Chem.* 18 (2001) 3929–3951.
- [22] F. Perez-Cruz, S. Vazquez-Rodriguez, M.J. Matos, A. Herrera-Morales, F.A. Villamena, A. Das, B. Gopalakrishnan, C. Olea-Azar, L. Santana, E. Uriarte, *Eur. J. Med. Chem.* 56 (2013) 6136–6145.
- [23] F. Chimenti, A. Secci, A. Bolasco, A. Chimenti, A. Granese, O. Befani, P. Turini, S. Alcaro, F. Ortuso, *Bioorg. Med. Chem. Lett.* 14 (2004) 3697–3703.
- [24] D. Secci, S. Carradori, A. Bolasco, P. Chimenti, M. Yanez, F. Ortuso, S. Alcaro, *Eur. J. Med. Chem.* 46 (2011) 4846–4852.
- [25] A. Hornick, A. Lieb, N.P. Vo, J.M. Rollinger, H. Stuppner, H. Prast, *Neuroscience* 197 (2011) 280–292.
- [26] P. Pelikan, M. Liska, M. Valko, M. Mazur, *J. Magn. Reson. A* 112 (1996) 9–15.
- [27] J. Telsler, J. Krzystek, A. Ozarowski, *J. Biol. Inorg. Chem.* 19 (2014) 297–318.
- [28] M. Valko, H. Morris, M. Mazur, J. Telsler, E.J.L. McInnes, F.E. Mabbs, *J. Phys. Chem. B* 103 (1999) 5591–5597.
- [29] D.R. Duling, *J. Magn. Reson. B* 104 (1994) 105–110.
- [30] S.C. Laskowski, R.O. Clinton, *J. Am. Chem. Soc.* 71 (1950) 3602–3606.
- [31] C. Holmes, P.N. Macher, J.R. Grove, L. Jang, J.D. Irvine, *Bioorg. Med. Chem. Lett.* 18 (2008) 3382–3385.
- [32] P. Jia, R. Sheng, J. Zhang, L. Fang, Q. He, B. Yang, Y. Hu, *Eur. J. Med. Chem.* 44 (2009) 772–784.
- [33] S. Butini, E. Guarino, G. Campiani, M. Brindisi, S.S. Coccone, I. Fiorini, E. Novellino, T. Belinskaya, A. Saxena, S. Gemma, *Bioorg. Med. Chem. Lett.* 18 (2008) 5213–5216.
- [34] G.L. Ellman, K.D. Courtney, V. Andres Jr., *Biochem. Pharmacol.* 7 (1961) 88–95.
- [35] www.graphpad.com.
- [36] R.B. Walker, J.D. Everette, *J. Agric. Food Chem.* 57 (2009) 1156–1161.
- [37] R. Re, N. Pellegrini, A. Proteggente, A. Pannala, M. Yang, C. Rice-Evans, *Free Radic. Biol. Med.* 26 (1999) 1231–1237.
- [38] M. Arts, G. Haenen, H. Voss, A. Bast, *Food Chem. Toxicol.* 42 (2004) 45–49.
- [39] M. Valko, D. Leibfritz, J. Moncol, M.T.D. Cronin, M. Mazur, J. Telsler, *Int. J. Biochem. Cell Biol.* 39 (2007) 44–84.
- [40] M. Zalibera, A. Stasko, A. Slobodová, V. Jancovicova, T. Cermakova, V. Brezova, *Food Chem.* 110 (2008) 512–521.
- [41] J. Peisach, W.E. Blumberg, *Arch. Biochem. Biophys.* 165 (1974) 691–708.

- [42] V. Brezova, M. Valko, M. Breza, H. Morris, J. Telser, D. Dvoranova, K. Kaiserova, L. Varecka, M. Mazur, D. Leibfritz, *J. Phys. Chem. B* 107 (2003) 2415–2425.
- [43] M. Valko, H. Morris, M.T.D. Cronin, *Curr. Med. Chem.* 12 (2005) 1161–1208.
- [44] S. Rahimpour, I. Bilkis, V. Peron, G. Gescheidt, F. Barbosa, Y. Mazur, Y. Koch, L. Weiner, *Photochem. Photobiol.* 74 (2001) 226–236.
- [45] S. Dorotikova, J. Koziskova, M. Malcek, K. Jomova, P. Herich, K. Plevova, K. Briestenska, A. Chalupkova, J. Mistrikova, V. Milata, D. Dvoranova, L. Bucinsky, *J. Inorg. Biochem.* 150 (2015) 160–173.
- [46] M. O'Connor, A. Kellett, M. McCann, G. Rosair, M. McNamara, O. Howe, B.S. Creaven, S. McClean, A.F. Kia, D. O'Shea, M. Devereux, *J. Med. Chem.* 55 (2012) 1957–1968.
- [47] B. Macías, I. García, M.V. Villa, J. Borrás, M. González-Álvarez, A. Castineiras, *J. Biochem.* 96 (2003) 367–374.
- [48] C.R. García, C. Avgelé-Martínez, J.A. Wilkes, H.C. Wang, E.E. Battin, J.L. Brumaghim, *Dalton Trans.* 41 (2012) 6458–6467.
- [49] G.A. Russel, *J. Am. Chem. Soc.* 79 (1957) 3871–3877.
- [50] J. Korabecny, K. Musilek, O. Holas, J. Binder, F. Zemek, J. Marek, M. Pohanka, V. Opletalova, V. Dohnal, K. Kuca, *Bioorg. Med. Chem. Lett.* 20 (2010) 6093–6095.
- [51] S. Hamulakova, L. Janovec, M. Hrabnova, K. Spilovska, J. Korabecny, P. Kristian, K. Kuca, J. Imrich, *J. Med. Chem.* 57 (2014) 7073–7084.
- [52] H. LeVine, *Protein Sci.* 2 (1993) 404–410.